

Article

Evaluating the Spectral and Physiological Responses of Grapevines (*Vitis vinifera* L.) to Heat and Water Stresses under Different Vineyard Cooling and Irrigation Strategies

Alessia Cogato ¹, Lihua Wu ², Shaikh Yassir Yousouf Jewan ^{2,3}, Franco Meggio ⁴, Francesco Marinello ¹, Marco Sozzi ¹ and Vinay Pagay ^{2,*}

- ¹ Department of Land, Environmental, Agriculture and Forestry, University of Padova, 35020 Legnaro, PD, Italy; alessia.cogato.1@phd.unipd.it (A.C.); francesco.marinello@unipd.it (F.M.); marco.sozzi@unipd.it (M.S.)
- ² Waite Research Institute, School of Agriculture, Food and Wine, The University of Adelaide, Glen Osmond, Adelaide, SA 5064, Australia; lihua0074@gmail.com (L.W.); shaikh.jewan@adelaide.edu.au (S.Y.Y.J.)
- ³ School of Biosciences, University of Nottingham Malaysia, Semenyih 43500, Selangor Darul Ehsan, Malaysia
- ⁴ Department of Agronomy, Food, Natural Resources, Animals and the Environment, University of Padova, 35020 Legnaro, PD, Italy; franco.meggio@unipd.it
- * Correspondence: vinay.pagay@adelaide.edu.au



Citation: Cogato, A.; Wu, L.; Jewan, S.Y.Y.; Meggio, F.; Marinello, F.; Sozzi, M.; Pagay, V. Evaluating the Spectral and Physiological Responses of Grapevines (*Vitis vinifera* L.) to Heat and Water Stresses under Different Vineyard Cooling and Irrigation Strategies. *Agronomy* **2021**, *11*, 1940. <https://doi.org/10.3390/agronomy11101940>

Academic Editors: Rita B. Santos and Andreia Figueiredo

Received: 3 September 2021

Accepted: 23 September 2021

Published: 27 September 2021

Publisher's Note: MDPI stays neutral with regard to jurisdictional claims in published maps and institutional affiliations.



Copyright: © 2021 by the authors. Licensee MDPI, Basel, Switzerland. This article is an open access article distributed under the terms and conditions of the Creative Commons Attribution (CC BY) license (<https://creativecommons.org/licenses/by/4.0/>).

Abstract: Heat stress (HS) and water stress (WS) pose severe threats to viticulture, and effective management solutions to counter their effects on grapevine performance must be examined. In this study, we evaluated the physiological and spectral responses of *Vitis vinifera* L. cv. Sauvignon blanc to individual (HS) and combined (HS + WS) stress under four different cooling and irrigation strategies. The treatments were: standard drip irrigation (SI), extra drip irrigation (SI+), extra sprinklers irrigation (SPRI), and sustained deficit irrigation (SDI; 50% of SI). Compared to the other treatments, in the early stages after the occurrence of HS, the vine water status of SPRI and SI+ improved, with high stomatal conductance (g_s) (SPRI) and stem water potential (Ψ_{stem} ; SPRI and SI+). All the physiological indicators measured were significantly lower after the end of HS in the SDI treatment. We also identified the spectral response of grapevine to HS and combined HS and WS (resulting from SDI). Consistent with the physiological analysis, the proximal spectral responses of leaves identified SPRI and SI+ as putative cooling strategies to minimize vine HS. The vines undergoing combined stress (SDI) showed greenness amelioration 10 days after stress, as revealed by the greenness vegetation indices (VIs), i.e., Green Index (GI), Normalized Difference Greenness Vegetation Index (NDGI), and Visible Atmospherically Resistant Index (VARI). However, their physiological recovery was not achieved within this time, as shown by the Simple Ratio Index (SRI), Transformed Chlorophyll Absorption Ratio Index (TCARI), and TCARI/Optimized Soil-Adjusted Vegetation Index (TCARI/OSAVI). A three-step band selection process allowed the identification of the spectral traits' responsive to HS and combined stress, i.e., 1336–1340 nm, 1967–1971 nm, and 600–604 nm.

Keywords: heat stress; drought stress; grapevine; vegetation indices; hyperspectral analysis; grapevine physiology

1. Introduction

One of the consequences of climate change is the increased frequency, duration and intensity of heatwaves [1,2]. Heatwaves, defined as the persistence of three or more days at or above 35 °C [3], are affecting viticultural areas globally, especially in Europe [4–6] and Australia [7,8]. Current projections estimate that heatwaves will further increase by 2100 [9,10].

The effects of heat stress (HS) on grapevine physiology have been studied. The inhibition of net photosynthesis (P_n) caused by HS can lead to lower yield in several

grapevine varieties [6,7]. Grape berry maturation may be delayed [11], with a consequent reduction in the size and fresh weight [7] and increased shriveling of berries [12,13]. A decoupling between anthocyanins and sugar was observed in Shiraz and Cabernet Franc under high-temperature conditions [14], and rotundone concentrations were reduced in Shiraz wines [15].

Given the environmental conditions of high temperature and low relative humidity (RH) that occur during a heatwave, if soil water is limited, HS is associated with water stress (WS), due to the increased evaporative demand [16]. WS affects the morphological traits (e.g., reduction in leaf size and vegetative growth) and physiological traits (e.g., reduction in P_n , stomatal conductance— g_s , and leaf transpiration rate— E) of vegetation [17]. Although moderate WS increases the quality of red varieties, e.g., promoting the accumulation of quality-related metabolites, it substantially reduces berry size and yield [18]. Moreover, WS may cause oxidative damage via the production of reactive oxygen species, which damage the cells and their components [19]. To date, less attention has been paid to the combined effects of HS and WS on grapevines. Some studies have underlined that the consequences of combined stresses may be substantially different from those of individual stresses. For example, combined HS and WS leads to increased leaf temperature due to stomatal closure, whereas during individual HS, heat is dissipated through stomata [20].

Application of evaporative cooling via sprinklers or drip irrigation may lead to an improvement in the soil water balance [21], improving vine water status and reducing HS. For example, small amounts of water distributed for three minutes every 15 min by overhead sprinklers lowered the ambient temperature around the canopy by 7 to 10 °C and raised the humidity from 10 to 20% in Tokay [22]. In-canopy misters reduced the canopy temperature of Sauvignon blanc and Cabernet Sauvignon grapevines by 5 °C [23].

Previous studies investigated the physiological response of grapevines to HS and WS under different water management schemes. Edwards et al. [24] studied the effects of a heatwave generated in a glasshouse on Cabernet Sauvignon physiology under regular and deficit irrigation. Their findings showed that g_s of deficit-irrigated vines was reduced by more than 85%, P_n by 30%, and internal CO₂ concentration (C_i) by 9%. Sousa et al. [25] analyzed the changes in several physiological parameters in Aragonês under different water regimes. Their results revealed that g_s , and E were significantly correlated with soil water content, and leaf water potential (Ψ_L) exhibited poorer performance compared to the previous indicators. On the contrary, Ψ_L was considered a good indicator of vine water status in Pinot noir under three water management strategies [26].

An accurate estimation of the physiological behavior of grapevine under stress conditions entails the use of complex and, in some cases, destructive equipment. Non-destructive techniques to quantify the effects of extreme weather events on crops are emerging using reflectance or spectral techniques [27]. For example, the green (550 and 570 nm), red (670 nm), red edge (>700 nm), and near-infrared (NIR, 800 nm) spectral bands can provide a reliable prediction of Carménère water status [28]. The NIR spectral band can provide a reliable assessment of the water status of leaves and canopy [29]. Environmental RH during HS correlated positively with the red edge region and growing degree days correlated negatively with the short wave near-infrared (SWIR, 1610 nm) region [3]. There are a wide range of spectral vegetation indices (VIs) used to describe WS, and some preliminary studies have been conducted on HS. Although a considerable number of studies have been carried out to assess the physiological and spectral responses of grapevine WS, specific knowledge of these responses under combined stresses and HS with different evaporative cooling systems is lacking. To the best of our knowledge, the validation of the spectral response with an accurate physiological analysis has not been performed.

In this study, three methods of evaporative cooling were investigated on *Vitis vinifera* L. cv. Sauvignon blanc under HS conditions in the Riverland region of South Australia. Moreover, a fourth treatment, namely sustained deficit irrigation, was evaluated. The specific objectives of this study were to: (i) evaluate the physiological responses to HS of *Vitis vinifera* L. cv. Sauvignon blanc under different cooling treatments, and the interactions with

WS; and (ii) identify the most consistent, robust, and reliable spectral predictors (hyperspectral bands and VIs) of the physiological responses to HS, and combined WS and HS, and the effects of various evaporative cooling systems. These objectives aimed at verifying our hypotheses that (i) evaporative cooling systems can minimize the physiological effects of HS; and (ii) spectral sensors can be used to assess the physiological responses of grapevines under HS and combined stresses. Testing hypothesis (i) may allow for decision making around management strategies, specifically evaporative cooling systems and irrigation, to reduce the adverse effects of HS on vine performance and grape/wine quality. Moreover, verifying hypothesis (ii) contributes to unravelling the poorly known effects of concurrent HS and WS on grapevines, and identifying non-destructive tools to assess HS in vineyards. Our study proposed a methodological approach that uses an integrated instrumental approach to analyze HS and combined HS and WS. Moreover, the study provided field results during a particularly critical season.

2. Materials and Methods

2.1. Study Area and Experimental Design

The study was conducted in January 2020 at Yalumba Oxford Landing Estate (OLE), a commercial vineyard (Figure 1) in the Riverland, South Australia ($34^{\circ}06'06.29''$ S and $139^{\circ}50'39.21''$ E). The vineyard block (0.9 ha) was planted in 1995 with *Vitis vinifera* L. cv. Sauvignon blanc, clone H10-F4V6, rootstock Ramsey, and was 100% mechanizable [30]. Rows were orientated N–S at a spacing of 1.8 m between vines and 3.0 m between rows (approx. 1852 vines ha^{-1}). The vines were trained to the Quadrilateral cordon training system, and their height was approximately 2.3 m. The topsoil layer (5–25 cm) was loamy sand, and the subsoil sandy loam to loamy sand. There are not known water tables in the top 3.5 m of the soil profile.

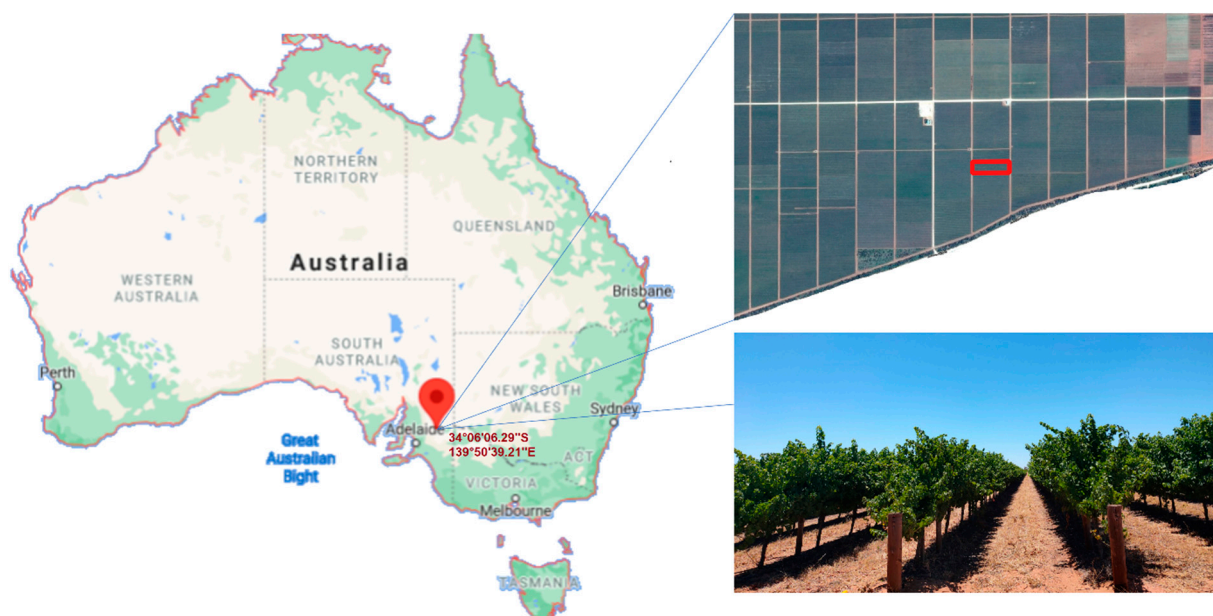


Figure 1. Identification of the study area.

The experimental design consisted of the implementation of four irrigation strategies with 24 replicate vines per treatment in a 3×3 Latin Square experimental design with at least two rows as buffer within treatments. Therefore, the total number of vines considered in this study was 96. The four treatments were:

1. Standard drip irrigation (SI)—conventional irrigation for the region, growers applied 4 h of additional irrigation during the day preceding HS. Irrigation was applied using a single dripline with pressure-compensating emitters spaced 0.3 m apart, each

with a flow rate of 1 L h^{-1} . This spacing and flow rate delivered approximately $6 \text{ L vine}^{-1} \text{ h}^{-1}$, 1.11 mm h^{-1} .

2. Extra drip irrigation (SI+)—same irrigation as SI and, in addition, four cycles of 30 min on/30 min off were triggered at night before HS. The treatment consisted of a separated irrigation line with two drippers per vine (flow rate: 13.5 L h^{-1}). The target flow rate was $54 \text{ L vine}^{-1} \text{ night}^{-1}$. The system was controlled with a Galcon G.S.I. DC power wireless solenoid controller.
3. Sprinkler irrigation (SPRI)—the treatment consisted of the same irrigation as SI, and, in addition, an under-vine broadcast sprinkler covering both the under-vine and inter-row regions. Timing and volume of water were the same as SI+. The system was controlled with a Galcon G.S.I. DC power wireless solenoid controller.
4. Sustained deficit irrigation (SDI)—50% of SI from approximately one week before HS (approximately two weeks post véraison) to harvest.

The additional amount of water in SI+ and SPRI was provided during the night to minimize evaporative losses from the soil.

In assessing soil/vine responses to deficit irrigation, the water balance method for estimating irrigation requirements is not considered an appropriate technique, and, instead, indicators based on plant water status have been recommended [31]. Therefore, the level of deficit irrigation implemented in SDI was assessed based on significantly different Ψ_{stem} .

2.2. Meteorological Data

The meteorological data (average and maximum daily air and soil temperature; average and minimum daily relative humidity; maximum daily vapor pressure deficit; average and maximum daily solar radiation) were obtained from an onsite automatic weather station (AWS) located approximately 1 km from the trial block. The station is part of the Natural Resources Management (NRM) weather station network, and data are accessible online (<https://www.awsnetwork.com.au/station/2770>, accessed on 1 March 2021).

The field campaigns took place between the 10 and 25 January 2020. The sampling dates were based on weather forecasts. The 10th of January was considered the reference date four days prior to the HS period, and post-HS was considered during two periods—two days (17 January; short-term recovery response) and 10 days (25 January; medium-term recovery response)—following the last HS day. HS occurred between 14th and 15th January, for two days, with average daily maximum and minimum temperatures during this period of 37.0 and 16.4 °C, respectively.

2.3. Physiological Measurements

During the experiment, the leaf physiological values of Ψ_{stem} , g_s , E , P_n , and intrinsic water use efficiency ($WUE_i = P_n/g_s$) were measured. These variables are considered relevant due to their prior response to water status [32–35] and HS [36]. Ψ_{stem} was measured on one leaf per vine, selecting one random mature, fully exposed, and healthy leaf. Leaf gas exchanges (g_s , E , P_n , and WUE_i), were measured on one leaf of the same shoot with the same characteristics.

Ψ_{stem} was measured using a Scholander-type pressure chamber (Model 1505D EXP, PMS Instruments, Albany, OR, USA). Before measurements, leaves were sealed for at least 60 min with an aluminum foil-coated plastic bag to stop transpiration. The measurements were performed within 30 s from cutting and always by the same operator to minimize human error. One leaf per vine was used for Ψ_{stem} measurements for a total of 96 observations for each of the three dates considered. The measurement was carried out within 1.5 h on each side of solar noon (13.30 h)

A portable infrared gas analyzer (IRGA, Model LI-6400XT, LI-COR, Lincoln, NE, USA) was used for instantaneous leaf gas exchange measurements of g_s , E , and P_n . The measurements were taken at environmental CO_2 concentration (Ref $\text{CO}_2 = 400 \text{ ppm}$), saturating radiation levels ($\text{PAR} = 1500 \mu\text{mol m}^{-2} \text{ s}^{-1}$), and flow rate of $500 \mu\text{mol s}^{-1}$ allowing RH in the leaf chamber ranging between 30–40%. The cuvette area was 6 cm^2 .

The measurements were carried out within 1.5 h at each side of solar noon (13.30 h) on one leaf per vine of one of the three replications, for a total of 32 observations (1/3 of the total sample) for each of the three dates considered.

2.4. Hyperspectral Measurements

The diffuse reflectance spectra were detected for one leaf per vine using a portable high-resolution spectrophotometer (ASD FieldSpec[®] 3, Analytical Spectral Devices, Boulder, CO, USA). The instrument records the full range solar irradiance spectrum (350–2500 nm) with a resolution of 3.5 nm in the visible-near infrared 350–1000 nm range, 10 nm in the 1000–1900 nm range, and 7 nm in the 1900–2500 nm range. The spectra collection was carried out using the default contact probe provided by the company, which allows using the ASD as an active sensor. The instrument is provided with the RS₃[™] dedicated software, which enables acquisition of the spectral signature of the leaves. The calibration of the instrument, which was used in reflectance mode, was performed by acquiring a white reference scan from a Spectralon[®] tile (Analytical Spectral Devices, Boulder, CO, USA). The dark reference was acquired using a closed cuvette without light.

A total of 96 hyperspectral measurements were made on the same vines characterized for Ψ_{stem} concurrently on each of the three dates. The reflectance was measured on one leaf per vine positioned in the same shoot of the leaves used for the physiological measurements.

The raw spectral data were imported into R statistical software (Version 3.5.2, RStudio Version 1.2.1335) to derive the VIs reported in Table 1. The VIs were selected after a literature survey. The VIs used in this study were classified into different categories. Most are greenness VIs, measuring the quantity and vigor of green vegetation (EVI, GI, GNDVI, MSR, NDGI, NDVI, SRI, TCARI, and VARI). PRI is a light use efficiency VI, providing an indication of the efficiency with which vegetation uses incident light for photosynthesis, and TCARI/OSAVI is a combination of indices designed to minimize soil background and leaf area index variation [37]. WBI is a canopy water content VI, which has been proven to track the changes in the relative water content of crops.

Table 1. Overview of the VIs used to assess WS and HS in grapevines.

Index	Formula	Stress	Cultivar	Reference
Normalized Difference Vegetation Index [38]	$\text{NDVI} = \frac{R_{800} - R_{670}}{R_{800} + R_{670}}$	WS	<i>Vitis vinifera</i> L. cv. Muscat, Carignan, Grenache Noir, Shiraz, Mourvedre, Petit Verdot	[39,40]
		WS	<i>Vitis vinifera</i> L. cv. Tempranillo	[41]
		WS	<i>Vitis vinifera</i> L. cv. Cabernet Sauvignon	[42]
		WS	<i>Vitis vinifera</i> L. cv. Carménère	[28]
		WS	<i>Vitis vinifera</i> L. cv. Chardonnay	[43]
		WS	<i>Vitis vinifera</i> L. cv. Thompson Seedless	[44]
		HS	<i>Vitis vinifera</i> L. cv. Sangiovese	[45]
Green Normalized Difference Vegetation Index [46]	$\text{GNDVI} = \frac{R_{800} - R_{550}}{R_{800} + R_{550}}$	WS	<i>Vitis vinifera</i> L. cv. Carménère	[28]
		WS	<i>Vitis vinifera</i> L. cv. Tempranillo	[41]
		WS	<i>Vitis vinifera</i> L. cv. Cabernet Sauvignon	[42]
Modified Simple Ratio [47]	$\text{MSR} = \frac{\frac{R_{800}}{R_{670}} - 1}{\sqrt{\frac{R_{800}}{R_{670}} + 1}}$	WS	<i>Vitis vinifera</i> L. cv. Tempranillo	[41]
		WS	<i>Vitis vinifera</i> L. cv. Carménère	[28]
Transformed Chlorophyll Absorption Ratio Index [48]	$\text{TCARI} = 3 * [(R_{700} - R_{670}) - 0.2 * (R_{700} - R_{550}) * (\frac{R_{700}}{R_{670}})]$	WS	<i>Vitis vinifera</i> L. cv. Tempranillo	[41]
		HS	<i>Vitis vinifera</i> L. several cultivars	[49]

Table 1. Cont.

Index	Formula	Stress	Cultivar	Reference
TCARI/Optimized Soil-Adjusted Vegetation Index [48]	$\text{TCARI/OSAVI} = \frac{3 * [(R_{700} - R_{670}) - 0.2 * (R_{700} - R_{550}) * (\frac{R_{700}}{R_{670}})]}{(1 + 0.16) * (R_{800} - R_{670}) / (R_{700} + R_{670} + 0.16)}$	WS	<i>Vitis vinifera</i> L. cv. Tempranillo	[41]
		WS	<i>Vitis vinifera</i> L. cv. Thompson Seedless	[44]
Green Index [49]	$\text{GI} = \frac{R_{554}}{R_{677}}$	WS	<i>Vitis vinifera</i> L. cv. Tempranillo	[41]
Simple Ratio Index 800/550 [50]	$\text{SRI} = \frac{R_{800}}{R_{550}}$	WS	<i>Vitis vinifera</i> L. cv. Tempranillo	[41]
Visible Atmospherically Resistant Index [51]	$\text{VARI} = \frac{R_{550} - R_{670}}{R_{550} + R_{670} - R_{470}}$	WS	<i>Vitis vinifera</i> L. cv. Touriga Nacional	[52]
Normalized Difference Greenness Vegetation Index [49]	$\text{NDGI} = \frac{R_{530} - R_{670}}{R_{530} + R_{670}}$	WS	<i>Vitis vinifera</i> L. cv. Touriga Nacional	[52]
Photochemical Reflectance Index [53]	$\text{PRI} = \frac{R_{530} - R_{550}}{R_{530} + R_{550}}$	WS	<i>Vitis vinifera</i> L. cv. Thompson Seedless	[44]
		HS	<i>Vitis vinifera</i> L., several cultivars	[3]
Enhanced Vegetation Index [54]	$\text{EVI} = 2.5 * \frac{R_{800} - R_{670}}{R_{800} + 6 * R_{670} + 6 * R_{470}}$	WS	Several crops (e.g., cotton, creosote bush, spruce)	[55]
		WS	<i>Vitis vinifera</i> L. cv. Chardonnay	[56]
		WS	<i>Vitis vinifera</i> L., several cultivars	[58]
Water Band Index [57]	$\text{WBI} = \frac{R_{950}}{R_{900}}$	WS	<i>Vitis vinifera</i> L., several cultivars	[58]

2.5. Data Analysis

2.5.1. Evaluation of the Treatments

The aim of the analyses was to test the hypothesis by comparing the vine performance under the four different treatments over three different dates: 10th of January, before HS; 17th and 25th of January, two and 10 days after the end of HS, respectively. The physiological data and VIs were used to compare the four treatments. Two-way ANOVA was performed using the GraphPad Prism 8.0.0 (GraphPad Software, Inc., La Jolla, CA, USA) software package. Means were separated by Tukey's Least Significant Differences (LSD) test. The null hypothesis for the statistical analysis was that there is no significant difference between the treatments over different dates ($p \leq 0.05$).

2.5.2. Optimum Hyperspectral Reflectance Bands Selection

The selection of the wavebands was based on the premise that the optimum bands are those that have the lowest autocorrelation, provide high information, and allow discrimination of the target [59,60]. To quantify these three assumptions, the analysis was carried out as follows.

First, the spectral regions between 350–399 nm, 1355–1420 nm, 1810–1940 nm and 2470–2500 nm were removed from analysis. These regions are considered to be noisy regions [59,61]. Then, the spectral regions that are more sensitive to HS under different cooling treatments were identified by plotting the percentage reflectance of each treatment relative to that of SI+, which was expected to be the most effective treatment.

SWIR and NIR spectral regions were also analyzed, because small reflectance differences in these spectral regions may correspond to strong differences in plant vigor caused by signal saturation [62]. Thus, spectral regions with a wavelength before 720 nm (red edge) were selected considering those with higher differences, whereas spectral regions beyond the red edge were investigated even if smaller differences were detected, considering the highest reflectance of plants in those spectral regions.

The bands pertaining to the areas of different spectral regions which exhibited higher differences from SI+ in all the other treatments were selected for further analysis.

Then, a band–band regression model was used. A high coefficient of determination (R^2) value between two bands implies redundant information, whereas a low R^2 value indicates that the two bands contain unique information, and thus are not auto-correlated (i.e., have low collinearity). For each band of spectral region identified in the previous step, the band pair correlations with the lowest R^2 were selected, leading to six band combinations. Principal component analysis (PCA) was carried out between the selected bands and the physiological parameters for each treatment. The PCA was implemented with the R statistical software (Version 3.5.2, RStudio Version 1.0.463) using the R package “FactoExtra” [63]. The aim was to analyze the importance of these bands for discriminating the different treatments. The band–band regression model was implemented with R statistical software, using the package “corr” [64] and selecting the pairs with the lowest R^2 .

To identify useful bands, further PCA was carried out using all the wavebands identified with the percentage reflectance plot. The bands were plotted against E rates measured two days after the end of HS, which showed the highest correlation with the spectral information and higher variability within the treatments. The five highest contribution bands of three principal components (PCs) were selected. The PCA was performed using the R statistical software.

Finally, Discriminant Analysis (DA) was performed to test the strength of data in discriminating the treatments. Due to the collinearity of many bands, it was not possible to run DA on original data, and data transformation did not improve the analysis. Therefore, DA was performed on twelve bands identified by the first three PCs of PCA and showing a Pearson’s correlation coefficient lower than $|0.700|$ [65,66]. The DA was carried out using the R package “klaR” [67] and splitting the dataset into training (80%) and test (20%) data. Figure 2 shows the conceptual selection model.

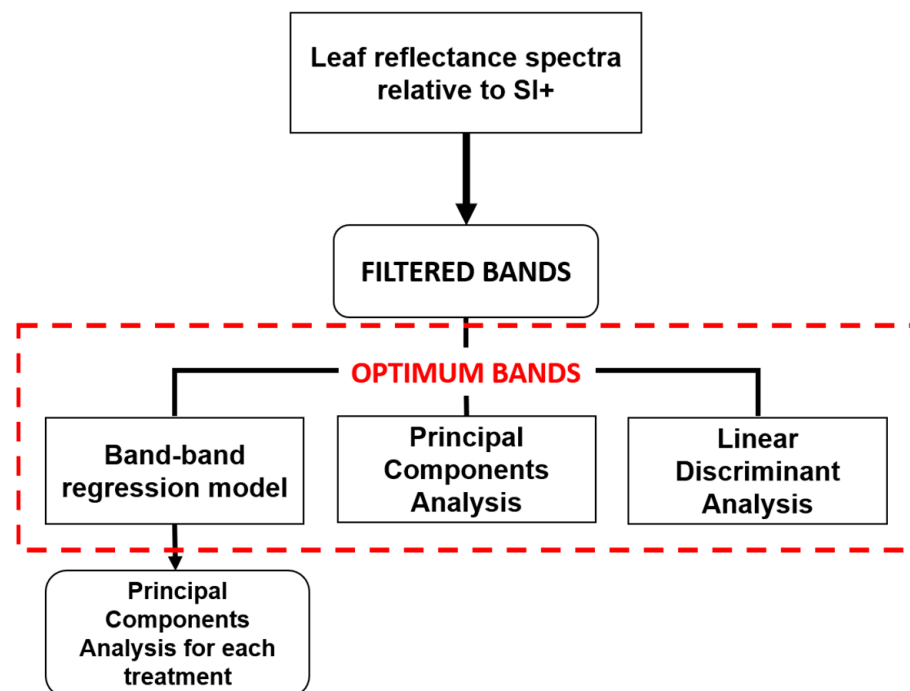


Figure 2. Conceptual model used for optimum bands selection.

3. Results

According to the AWS, on the 14 and 15 January 2020, the maximum temperature in the study area was above 35 °C. Although this could not be considered a heatwave, the vines experienced HS. When the air temperature exceeds 35 °C, key physiological processes of grapevines are compromised [68]. Detailed statistics on weather conditions that occurred on the 14th and 15th of January 2020 are reported in Table 2.

Table 2. Environmental conditions during the HS in the study area.

Date	Avg Daily T ^a (°C)	Max Daily T ^a (°C)	Avg Daily RH ^a (%)	Min Daily RH ^a (%)	Avg Daily Soil T ^{a,b} (°C)	Max Daily Soil T ^{a,b} (°C)	Max Daily VPD ^a (kPa)	Avg SR ^a (W m ⁻²)	Max SR ^a (W m ⁻²)
14 January 2020	26.2	35.4	38.1	12.6	43.5	80.6	2.1	371	1078
15 January 2020	27.0	39.0	47.3	12.6	49.6	89.9	1.9	339	1045
16 January 2020	21.0	33.3	54.9	0.0	46.2	80.6	1.12	356	1090

^a T = ambient temperature, RH = ambient relative humidity, soil T = soil temperature, VPD = vapor pressure deficit, SR = solar radiation; ^b soil temperature sensors were deployed approximately two meters from the weather station in unaltered site soils to a depth of 150 mm.

3.1. Grapevine Physiological Status: Water Relations and Gas Exchange

The physiological indicators of the treatments were compared using a two-way ANOVA (Figure 3).

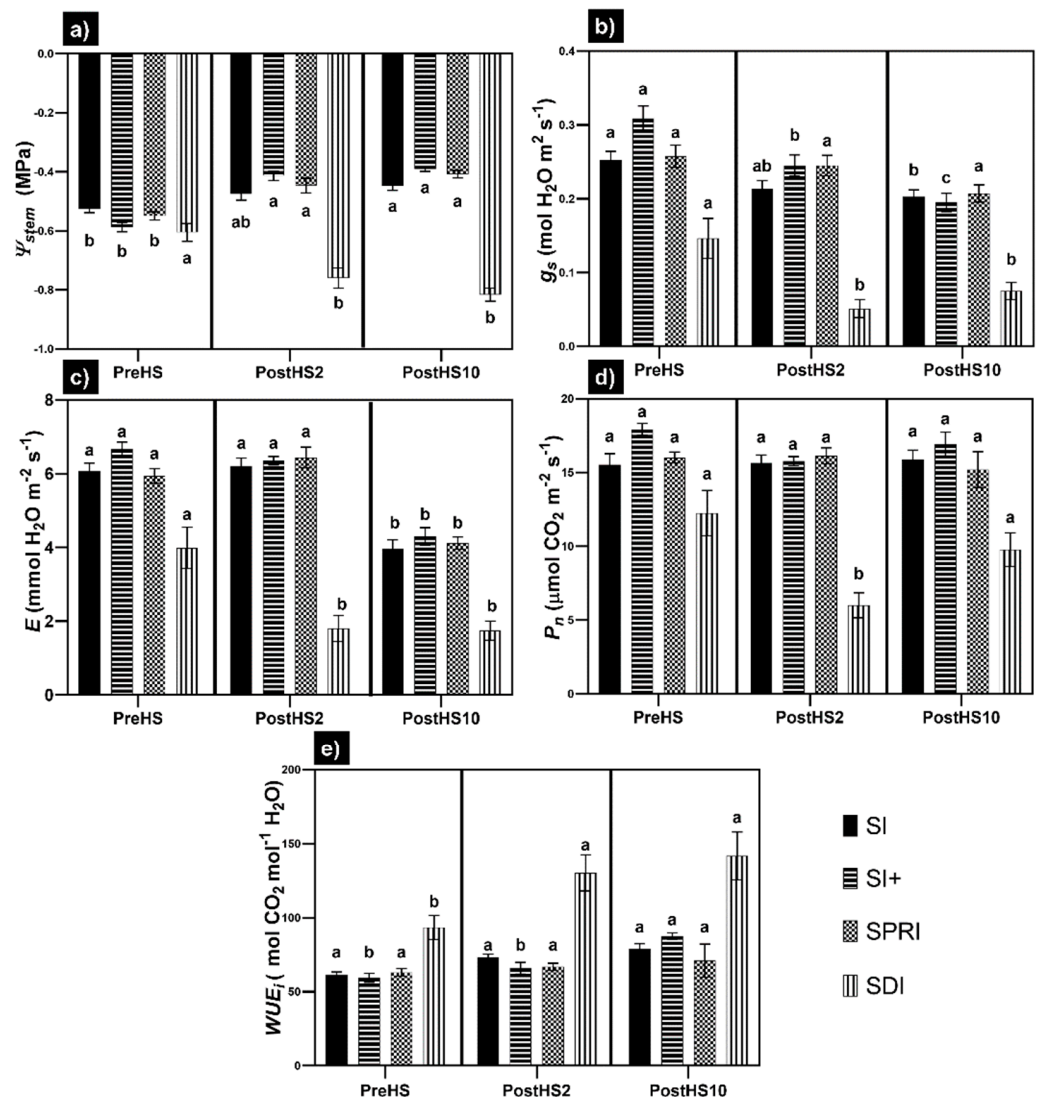


Figure 3. Variation in (a) stem water potential (Ψ_{stem}), (b) leaf stomatal conductance (g_s), (c) leaf net transpiration rate (E), (d) photosynthesis (P_n), and (e) leaf intrinsic water use efficiency (WUE_i) for Sauvignon blanc subjected to HS under different cooling treatments. Each data point is the mean \pm standard error of the mean of twenty-four (Ψ_{stem}) or eight (g_s , E , P_n , and WUE_i) replicates. The comparison dates were before HS (PreHS), two days after HS (PostHS2) and ten days after HS (PostHS10). Treatments sharing the same letter do not differ statistically at $p \leq 0.05$. Means were separated by two-way ANOVA using Tukey's Least Significant Difference (LSD) test.

Two days after the end of HS, Ψ_{stem} of two treatments (SI+ and SPRI) were higher than before HS (+29.7 and +25.8%, respectively). The same trend continued 10 days after the end of HS. SI did not show significantly different Ψ_{stem} values two days after the end of HS, but Ψ_{stem} significantly improved 10 days after the end of HS compared to the 10th of January, before HS (+14.7%). Ψ_{stem} of SDI showed a significant drop two days after the end of HS (−25.6%), which persisted 10 days after the end of HS (−34.8%).

The only treatment which maintained constant g_s over time was SPRI. The values of g_s did not show significant differences two days after the end of HS under SI but dropped after 10 days (−19.8% compared to before HS). SI+ showed a constant decrease in g_s (−20.6% and −36.8% two and 10 days after the end of HS, respectively). Under SDI, g_s dropped significantly two days after the end of HS (−65.0%), and, despite a slight recovery, stayed at a low level 10 days after the end of HS.

The trend of E was the same for three treatments (SI+, SPRI, and SI) with a significant decrease only 10 days after the end of HS. Conversely, E dropped in SDI immediately after HS (−54.8%), and the difference persisted 10 days after the end of HS.

Three treatments (SI+, SPRI, and SI) did not show any differences in P_n . Only SDI exhibited lower P_n rates two days after the end of HS (−51.0%) but recovered 10 days after the end of HS.

With regards to WUE_i , SPRI and SI did not show any significant change after HS. WUE_i was higher 10 days after the end of HS for SI+ (+47.8%). A significant increase was registered for SDI starting from two days after the end of HS (+39.5%) and persisted 10 days after the end of HS (+51.8%). Detailed information on the relative differences of the physiological parameters from the date before HS are reported in the Supplementary Materials (Table S1).

3.2. Hyperspectral-Derived VIs

With regards to the greenness VIs (Figure 4), in SI, EVI showed a significant difference 10 days after HS; GNDVI, MSR, NDVI, SRI, and TCARI were not affected by HS; GI, NDGI, and VARI showed a significant amelioration 10 days after HS. In SI+, EVI, MSR, and NDVI were significantly different 10 days after HS, but GI, GNDVI, NDGI, and VARI exhibited significant amelioration 10 days after HS. In SPRI, EVI, MSR, and NDVI showed a significant difference 10 days after HS, whereas GI, GNDVI, NDGI, SRI, and TCARI were not affected by HS. In SDI, most of the VIs exhibited lower performance immediately after HS, but GI and NDGI recovered 10 days after HS.

The remaining VIs showed different behavior (Figure 5). In SI, they did not show significant differences after HS. In SI+, PRI was significantly different from previous dates 10 days after the end of HS, whereas TCARI/OSAVI and WBI did not exhibit significant changes. In SPRI, PRI and WBI showed a significant difference 10 days after HS, and TCARI/OSAVI was not affected. In SDI, PRI was significantly lower two days after the end of HS and completely recovered 10 days after the end of HS; TCARI/OSAVI was significantly higher two days after the end of HS, with partial recovery 10 days after the end of HS; WBI showed a slight inflection immediately after HS, but was not significantly different from before HS. Subsequently, WBI started to recover. Detailed information on the relative differences in the VIs from the date before HS are reported in the Supplementary Materials (Table S2).

3.3. Optimum Bands Selection

The spectrum was filtered to identify the spectral regions more sensitive to HS, and the percentage reflectance of each treatment relative to that of SI+ was analyzed. The visual assessment allowed the selection of 520–610 nm (green), 620–640 nm (red), 680–720 nm (red edge), 770–1340 nm (NIR), 1421–1550 nm (SWIR), and 1941–2200 nm (water absorption bands) for further analysis (Figure 6).

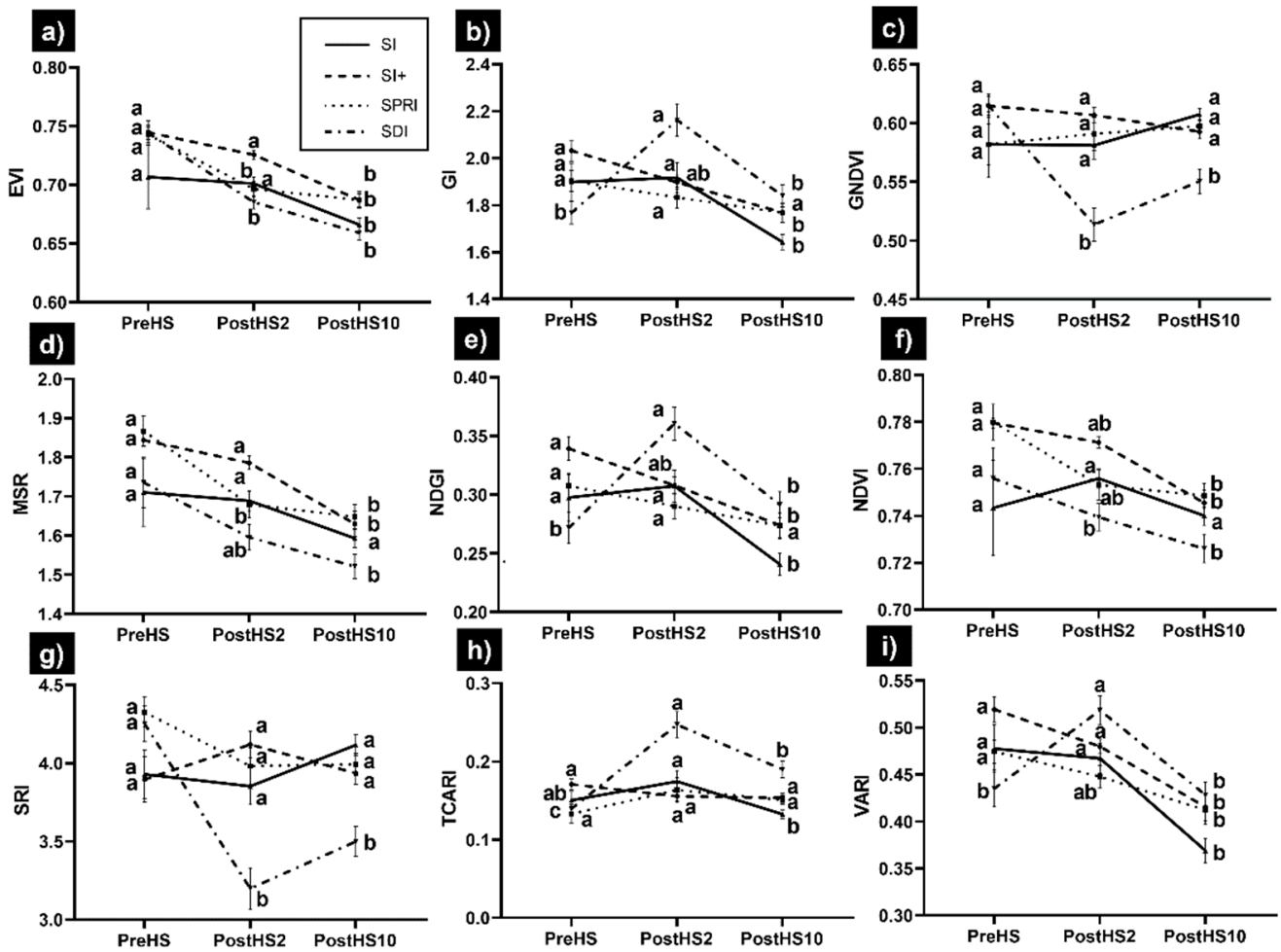


Figure 4. Variation in greenness vegetation indices for Sauvignon blanc subjected to HS under different cooling and water deficit treatments: (a) EVI, (b) GI, (c) GNDVI, (d) MSR, (e) NDGI, (f) NDVI, (g) SRI, (h) TCARI, (i) VARI. Each data point is the mean ± standard error of the mean of twenty-four replicates. The comparison dates were before HS (PreHS), two days after HS (PostHS2), and ten days after HS (PostHS10). Treatments sharing the same letter do not differ statistically at $p \leq 0.05$. Means were separated by two-way ANOVA using Tukey’s Least Significant Differences (LSD) test.

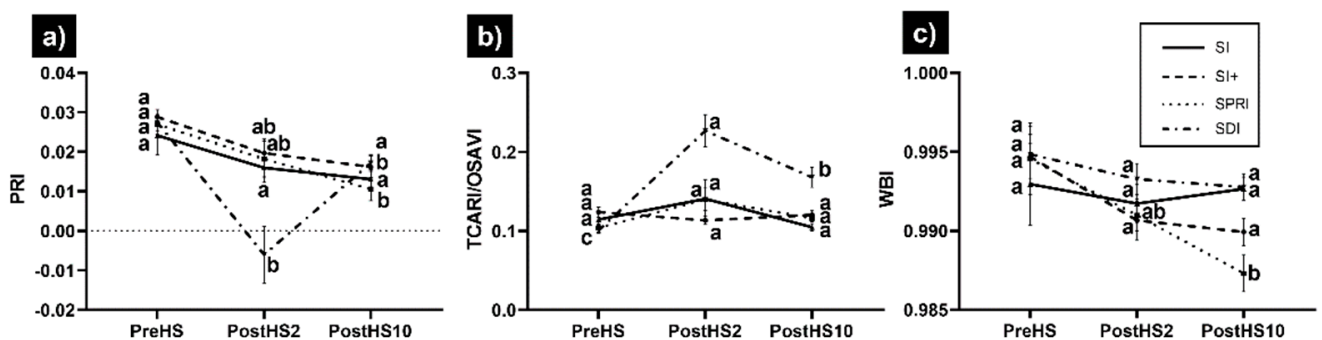


Figure 5. Variation in (a) PRI, (b) TCARI/OSAVI, and (c) WBI for Sauvignon blanc subjected to HS under different cooling treatments. Each data point is the mean ± standard error of the mean of twenty-four replicates. Treatments sharing the same letter do not differ statistically at $p \leq 0.05$. Means were separated by two-way ANOVA using Tukey’s Least Significant Differences (LSD) test.

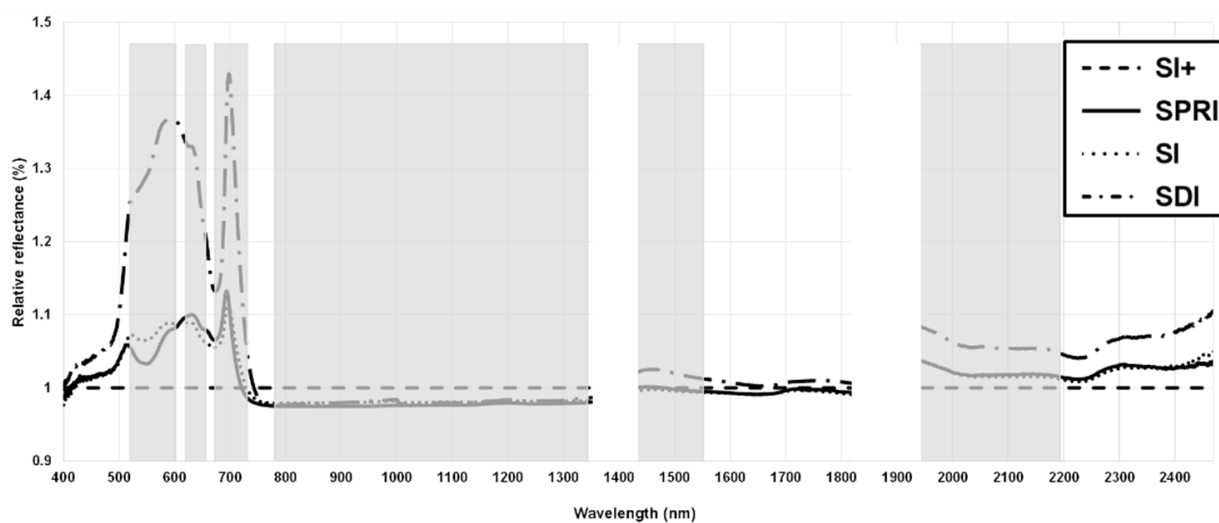


Figure 6. Visual spectral region filtering. Empty areas represent noisy regions, which were excluded from the analysis. Areas of the spectra highlighted grey were selected for further analysis.

The filtered bands were further investigated with a three-step process, including a band–band regression model, PCA, and DA. The band–band regression model revealed five pairs of bands that showed a very low coefficient of determination ($0.001 \leq R^2 \leq 0.203$, $p \leq 0.05$), thus providing unique information (Table 3). The most frequently occurring wavebands with low R^2 in the correlation matrix included the wavelengths pertaining to NIR (770–1340 nm) and the water absorption bands (1941–2200 nm). However, the selection of the band pairs aimed to include all the spectral regions identified with the relative reflectance filtering process (Figure 6): green, red, red edge, NIR, SWIR, and water absorption bands. Therefore, once the pairs with the coefficient of determination within the aforementioned range were identified, some were excluded based on their redundancy (bands similar to other pairs). The examination of the lowest R^2 bands with a PCA for each treatment allowed recognition of the best predictors of physiological status under HS (Figure 7). Overall, SI+, SDI, and SI performed similarly, with the water absorption bands (1496, 1948, 1952, and 2032 nm) negatively correlated with P_n , E , and g_s due to their location in the opposite quadrant, and a second group of wavebands (570, 604, 636, 720, 1000, and 1033 nm) with a weaker correlation to the physiological parameters. However, in contrast to the positive correlation between Ψ_{stem} and water absorption bands in SI+, the correlation was negative for SDI and SI. Furthermore, in SPRI, not only Ψ_{stem} , but also g_s had a positive correlation with water absorption bands and the red band (636 nm).

Table 3. Band combinations with the lowest R^2 .

Bands	R^2
570~2032	0.182
636~1000	0.184
720~1948	0.082
1333~1952	0.001
1496~604	0.203

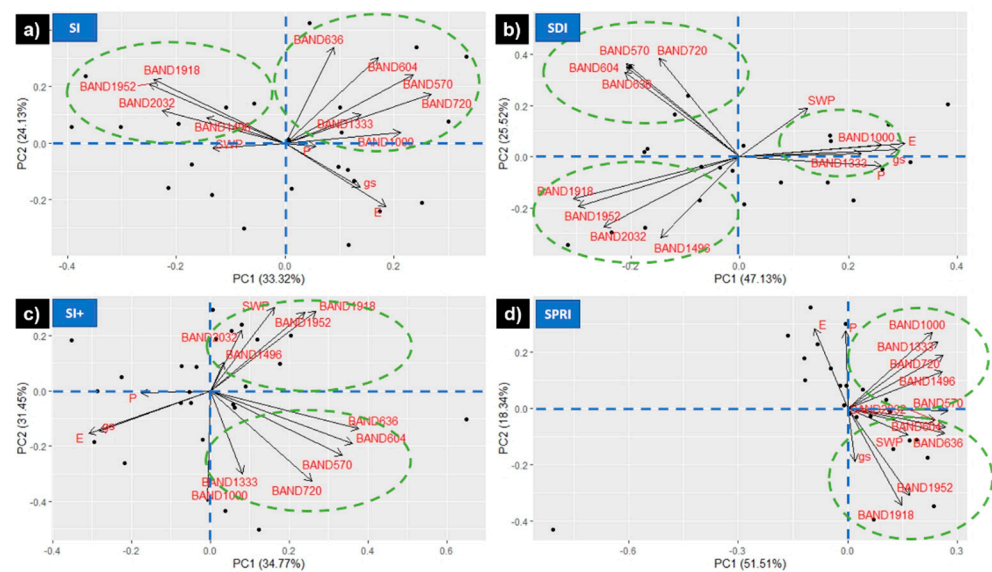


Figure 7. PCA of the wavebands selected with the band–band regression model and the physiological parameters (E = leaf transpiration rate, g_s = leaf stomatal conductance, P_n = net photosynthesis, SWP = stem water potential) for the four treatments. (a–d) represent different cooling and irrigation strategies, respectively.

The second step for band selection was PCA, which aimed to reduce 1013 wavebands to 15 critical bands, and enabled identification of three main spectral regions. The results showed that PC1, PC2, and PC3 were dominated by bands pertaining to NIR, water absorption bands, and the transition region between green and red bands. The first five contributing bands for each PC are displayed in Table 4.

Table 4. Results of the PCA on the filtered (1013) wavebands. The first row shows the top five bands of the first three components. The second row shows the top four bands for each component showing a Pearson’s correlation coefficient lower than $|0.700|$. These bands were used in the DA model.

Bands with Highest Factor Loading			Variability Explained (%)		
PC1	PC2	PC3	PC1	PC2	PC3
1340, 1339, 1338, 1337, 1336	1969, 1970, 1968, 1967, 1971	604, 603, 601, 600, 602	62.62	27.00	7.88
1340, 1550, 2199, 720	1969, 1440, 883, 610	604, 1924, 2010, 1338			

DA was inconclusive because it did not allow further discrimination between the twelve input variables. However, the twelve bands had reasonable potential to allow discrimination of the treatments (Wilk’s lambda = 0.47).

4. Discussion

Between December 2019 and January 2020, the study area suffered from repeated days of HS. We examined the HS days between the 14th and the 16th of January. During these days, the maximum temperature exceeded 35 °C for the first two days and remained high on the third day (Table 2). Temperature in excess of 35 °C compromises grapevine maximum P_n and g_s rates [68,69]. Thus, we tested the potential of different cooling systems to counter HS and the spectral responses of the vines under combined WS and HS, because premium vineyards for wine grapes are often deficit irrigated.

4.1. Which Cooling Was the Most Effective in Mitigating HS?

SI, SI+, and SPRI were applied to counter HS. SI provided 6–7 ML ha⁻¹ per season, which is typical of highly productive vineyards in this region. Based on whole canopy gas exchange measurements, these grapevines require approximately 40 L vine⁻¹ day⁻¹, whereas they were irrigated at approximately 20–25 L vine⁻¹ day⁻¹ [70]. By comparison, SI+ and SPRI proved to influence RH and reduce VPD inside the canopy without changing soil moisture [23]. The different levels of HS under different cooling systems were assessed by comparing physiological status indicators using ANOVA.

The results showed that SDI treatment suffered from HS, because all the physiological indicators were significantly lower two days after the end of HS, and the stress condition persisted 10 days after the end of HS (Figure 3). The analysis of Ψ_{stem} allowed for the quantitation of WS in SDI. Although the value of Ψ_{stem} before HS in SDI was not extremely low ($-0.63 \text{ MPa} \pm 1.6 \text{ MPa}$), this value was significantly different from that of the other treatments. The value of Ψ_{stem} recorded in SDI was consistent with a WS condition during the post-fruit set stage [71]. Moreover, Ψ_{stem} further decreased after HS (Figure 3a), indicating the concurrence of WS in SDI. The overall decline experienced under HS, characterized by physiological parameters, indicates a water conservation response [72]. The closure of stomata to limit water losses is one of the first reactions to WS, thus decreasing g_s and Ψ_{stem} . Stomatal control allows regulation of P_n and E , preserving vines from irreversible damage [73]. In the early phenological stages, the reduction in Ψ_{stem} induced by WS often coincides with reduced leaf area [74]. The limited photosynthetic area entails the decline in P_n . Furthermore, drought-induced closure of stomata is commonly associated with increased WUE_i values. Therefore, Ψ_{stem} , P_n , E , g_s , and WUE_i are physiological traits commonly associated with WS.

The analysis of Ψ_{stem} (Figure 3a) proved that SI+ and SPRI, the treatments which were supplied with more water during HS days, improved their performance after HS. SI also showed a higher Ψ_{stem} 10 days after the end of HS. Ψ_{stem} is considered a reliable index of water status in *Vitis vinifera*, and its values are the combination of different factors, such as VPD, soil water availability, stomatal regulation, and plant hydraulic conductivity [75,76].

Many studies have found that Ψ_{stem} and E rates decrease after HS, whereas the findings related to g_s behavior are controversial, because it is difficult to isolate the direct effect of temperature on g_s [77–79]. In the current study, g_s decreased significantly after HS, not only in SDI, but also in SI+ and SI, and persisted for up to 10 days after the end of the HS event (Figure 3b). In SPRI, g_s did not exhibit significant variation after HS, thus leading to the conclusion that HS causes stomatal closure in Sauvignon blanc, and SPRI treatments did not undergo HS. Under HS conditions, E remained initially high for the evaporative cooling treatments, thereby maintaining a relatively constant canopy temperature via evaporative cooling, but dropped rapidly for SDI (Figure 3c), thus highlighting the severe effect of combined HS and WS [80,81]. However, all treatments showed lower E 10 days after HS, probably due to higher average RH. In agreement with the findings of Luo et al. [82], HS at 35 °C did not significantly inhibit P_n , with the exception of SDI (Figure 3d). HS results in a trade-off between hydraulic function and leaf temperature, i.e., opening stomata to transpire under HS may compromise hydraulics and generate WS, whereas closing stomata may increase the leaf temperature to the point that P_n drops off [83]. Moreover, during HS, light energy usually absorbed by chlorophyll for photochemistry is partially lost as sensible heat [84]. Furthermore, there is a build-up of toxic reactive oxygen species inside the photochemical apparatus of the leaves, which can be quenched by heat dissipation mechanisms such as non-photochemical quenching. Finally, HS induces the biosynthesis of heat stress proteins (HSPs), which represents a vital adaptive mechanism. Nevertheless, the energy spent by the vines for the synthesis of HSPs has negative repercussions on yield [85]. The significant decrease in P_n only in SDI may confirm the potential efficiency of cooling systems in the other treatments.

According to the primary studies on grapevines under HS conditions, P_n , g_s , E , and Ψ_{stem} decreased sharply [24,78,86]. In this study, only SDI showed a decreasing trend for all

of the former physiological parameters, whereas SI+ and SPRI showed higher Ψ_{stem} . This response may confirm that the evaporative cooling systems had a positive effect on the mitigation of HS effects, with SPRI and SI+ performing slightly better than SI. Therefore, the cooling systems evaluated in this study may represent effective tools to counteract the negative influence of the heatwaves on vine physiological performance.

4.2. Which Is the Spectral Behavior of the Vines under Combined WS and HS?

Overall, the behavior of the VIs confirmed from the spectral perspective the observations in the physiological parameters (Figures 5 and 6).

Two days after the end of HS, SDI significantly differed both from pre-HS and from the cooling treatments. An exception was WBI, which was not capable of combined stress in SDI (Figure 5c). Because changes in leaf water content only occur during late stages of dehydration [87], the failure of WBI to detect vines stress suggests that the vines experienced moderate WS, and that WBI can be excluded from VIs for early tracking of combined stress. The analysis of the percentage difference in physiological parameters and VIs two and 10 days after the end of HS (see Supplementary Materials) allowed the identification of some trends. Specifically, GI, NDGI, and VARI showed that HS affected only the SDI treatment, but their values recovered to initial (pre-HS) levels within 10 days after the end of HS. Concurrently, SI+ and SI treatments showed an improvement 10 days after the end of HS, which may be related to their cooling efficacies. GI, NDGI, and VARI are greenness indices, which combine the green and red bands to account for dry vegetation, and have been proven to be effective for estimating drought stress [88] and leaf water potential [89]. In this study, the performance of GI, NDGI, and VARI was consistent with that of Ψ_{stem} and P_n . The spectral bands included in the equation of these VIs pertain to the visible domain, whose reflectance is influenced by pigment content [51]. The pigment content is related to HS, i.e., increased carotenoids and decreased Chlorophyll a and b content [90]. Therefore, the findings of this study suggest that the evaporative cooling systems mitigated physiological stresses associated with HS. In comparison, SRI, TCARI, and TCARI/OSAVI revealed a slightly different situation, with SDI still declining soon after HS, but not recovering even 10 days after the end of HS. Concurrently, the other treatments did not exhibit any significant change. Compared with the previous group of VIs, the VIs belonging to this second group contain the NIR (SRI) and/or red edge (TCARI and TCARI/OSAVI) bands. The reduction in water content after WS leads to a decreased NIR reflection. In previous studies, SRI has been used to assess vineyard water status [37,41]. Moreover, NIR has been previously shown to discriminate HS and estimate E [3]. VIs calculated in the red-edge spectral region were even more sensitive than NIR in the identification of temperature- and water-induced changes in Cabernet Sauvignon [91]. The failure of recovery of these VIs may indicate that, despite greenness and vigor amelioration, the physiological parameters could not recover as quickly after the combination of HS and WS. This hypothesis was supported by the fact that P_n and WUE_i showed the same trend as SRI, TCARI, and TCARI/OSAVI (Supplementary Materials). The third group of VIs (MSR, NDVI, and EVI) yielded slightly different and heterogeneous results, yet captured the effect of HS on SDI. Indices of the latter group result from a combination of red and NIR bands. Previous studies showed a difference of less than 1.0% in red reflectance for grapevines under HS conditions [91]. Our results suggest that VIs containing a combination of green, NIR, and red edge bands may help to track combined WS and HS in grapevines.

The three-step band selection process (band–band regression, PCA, and DA) aimed at providing complementary information by eliminating redundant bands (band–band regression and PCA), identifying the bands which drive vine response to WS and HS (PCA), and highlighting the bands which discriminate the treatment (DA). The first three PCs of PCA (Table 4) showed that the spectral regions involved in the vine response to HS were NIR (1336–1340 nm), water absorption bands (1967–1971 nm), and the transition region between green and red bands (600–604 nm). Compared to SI+, the other treatments

responded to HS by increasing the reflectance in the green/red and NIR regions, while decreasing it in the region of the water absorption bands (Figure 5). The 550–680 nm and red-edge bands are indicators of chlorophyll content at the leaf level [84,92]. The reflectance in the spectral region around 1240–1450 nm is influenced by leaf water content [93,94]. Consistent with the VI analysis, our findings indicate that two physiological processes— P_n and E —show the highest sensitivity to HS.

Band–band regression allowed for the determination of specific bands within each spectral region, which provided meaningful information about HS (Table 3). Some of the information provided by band–band regression was confirmed by PCA. Specifically, bands 604, 720, and 1333–1340 nm were recurrent in both analyses. Bands 1496, 1948, 1952, and 2032 nm showed a strong inverse correlation with P_n and E for all treatments, whereas g_s was directly correlated with these bands for SPRI and inversely correlated for the other treatments. Some of the aforementioned bands (604, 1496, 1948, and 1952 nm) are known to be sensitive to leaf water content [28,95,96]. Another difference indicated by the PCA of the lowest correlation bands was the direct correlation of bands 1000 and 1333 nm with the physiological indicators— Ψ_{stem} , g_s , P_n , and E —for SDI (Figure 7b). This finding suggests that NIR is the critical spectral region for detection of the combined effects of HS and WS.

5. Conclusions

In this study, we analyzed the physiological behavior of Sauvignon blanc under conditions of individual HS and combined HS and WS. Moreover, we compared the effectiveness of different evaporative cooling systems to mitigate HS. Finally, we tested the hypothesis that hyperspectral reflectance and derived VIs can provide effective and valuable information on grapevine response to HS conditions, and in combination with WS. Our main findings were:

- Combined HS and WS led to unsatisfactory Ψ_{stem} , g_s , P_n , E , and WUE_i values, which did not recover within 10 days.
- The cooling systems evaluated in the present study were efficacious in mitigating the adverse effects of HS. Specifically, SI+ and SPRI exhibited higher Ψ_{stem} after HS. Moreover, in SI+, P_n was not affected by HS in cooled vines, and in SPRI, both P_n and g_s were unaffected.
- The spectral VIs showed that SI+, SPRI, and SI were rapidly able to recover the greenness and vigor, as shown by GI, NDGI, and VARI.
- The vine physiological function did not completely recover even 10 days after HS with SRI, TCARI, and TCARI/OSAVI significantly different than their values before HS. The lack of full recovery may indicate that the VIs were sensitive to changes in g_s .
- The spectral regions more sensitive to HS were NIR (770–1340 nm), water absorption bands (1941–2200 nm), and the transition region between the green and red bands (600–604 nm), with NIR having the ability to discriminate between SDI and the cooling treatments.
- The single wavebands most sensitive to HS were 604, 720, and 1333–1340 nm.
- The hyperspectral data were consistent with physiological data, identifying SDI as the worst-performing treatment under HS, and SI+ and SPRI as effective cooling strategies to cope with HS.

In the current climate change context, vineyards are likely to increasingly experience HS, and farmers need to be supported with managing strategies. Scientific research has yet to devote sufficient attention to the effects of HS, and combined HS and WS, on vineyards. The physiological behavior of grapevines under HS still needs to be determined, and further study will be needed on different varieties, conditions, and areas before obtaining a comprehensive understanding of the topic. The measurement of physiological parameters with conventional methods is time consuming and tedious, particularly during hot days. The opportunity to replace these measurements with spectral assessments, either from proximal or remote instrumentation, would represent an effective and rapid tool to monitor environmental stresses in the field. Therefore, the findings and the methodology proposed

in this study contribute to expanding the knowledge of the effects of HS, and combined HS and WS, and the tools for future investigation.

Moreover, we explored the effectiveness of different evaporative cooling systems to help farmers cope with the adverse effects of HS. The findings may promote the implementation of vineyard irrigation strategies to ensure sustainable and profitable production.

Supplementary Materials: The following are available online at <https://www.mdpi.com/article/10.3390/agronomy11101940/s1>, Table S1: Differences in physiological parameters compared to the values before HS. Single asterisk indicates a significant difference, $p < 0.05$; double asterisk indicates a statistical difference, $p < 0.01$; triple asterisk indicates a statistical difference, $p < 0.001$; ns indicates no significant difference ($p > 0.05$), Table S2: Differences in VIs compared to the values before HS. Single asterisk indicates a significant difference, $p < 0.05$; double asterisk indicates a statistical difference, $p < 0.01$; triple asterisk indicates a statistical difference, $p < 0.001$; ns indicates no significant difference ($p > 0.05$).

Author Contributions: Conceptualization, A.C. and V.P.; methodology, A.C., V.P.; software, A.C., V.P. and S.Y.Y.J.; validation, F.M. (Francesco Marinello) and F.M. (Franco Meggio); formal analysis, A.C., S.Y.Y.J. and L.W.; investigation, A.C., S.Y.Y.J. and L.W.; data curation, A.C. and L.W.; writing—original draft preparation, A.C.; writing—review and editing, A.C., V.P., F.M. (Francesco Marinello), F.M. (Franco Meggio), M.S. and S.Y.Y.J.; supervision, V.P. All authors have read and agreed to the published version of the manuscript.

Funding: This research received no external funding.

Data Availability Statement: All the data generated or analyzed during this study are included in this published editorial.

Acknowledgments: The authors would like to thank Yalumba Oxford Landing Estate for providing the trial site and for vineyard management.

Conflicts of Interest: The authors declare no conflict of interest.

References

1. Arneth, A.; Barbosa, H.; Benton, T.; Calvin, K.; Calvo, E.; Connors, S. Summary for policymakers. In *Climate Change and Land: 602 an Ipcc Special Report on Climate Change, Desertification, Land Degradation, Sustainable Land Management, Food Security, and Greenhouse Gas Fluxes in Terrestrial Ecosystems*; IPCC: Geneva, Switzerland, 2019.
2. Perkins-Kirkpatrick, S.; Pitman, A. Extreme events in the context of climate change. *Public Health Res. Pract.* **2018**, *28*, 2–5. [[CrossRef](#)]
3. Cogato, A.; Pagay, V.; Marinello, F.; Meggio, F.; Grace, P.; Migliorati, M.D.A. Assessing the feasibility of using Sentinel-2 imagery to quantify the impact of heatwaves on irrigated vineyards. *Remote Sens.* **2019**, *11*, 2869. [[CrossRef](#)]
4. Bucur, G.M.; Babes, A.C. Research on trends in extreme weather conditions and their effects on grapevine in Romanian viticulture. *Bull. UASVM Hort.* **2016**, *73*, 126–134.
5. Duchêne, E.; Huard, F.; Dumas, V.; Schneider, C.; Merdinoglu, D. The challenge of adapting grapevine varieties to climate change. *Clim. Res.* **2010**, *41*, 193–204. [[CrossRef](#)]
6. Carvalho, L.; Coito, J.L.; Gonçalves, E.M.F.; Chaves, M.M.; Amâncio, S. Differential physiological response of the grapevine varieties Touriga Nacional and Trincadeira to combined heat, drought and light stresses. *Plant Biol.* **2015**, *18*, 101–111. [[CrossRef](#)] [[PubMed](#)]
7. Greer, D.H.; Weedon, M.M. The impact of high temperatures on vitis vinifera cv. semillon grapevine performance and berry ripening. *Front. Plant Sci.* **2013**, *4*, 1–9. [[CrossRef](#)]
8. Liang, L.; Sun, Q.; Luo, X.; Wang, J.; Zhang, L.; Deng, M.; Di, L.; Liu, Z. Long-term spatial and temporal variations of vegetative drought based on vegetation condition index in China. *Ecosphere* **2017**, *8*, e01919. [[CrossRef](#)]
9. Cowan, T.; Purich, A.; Perkins-Kirkpatrick, S.; Pezza, A.; Bosch, G.; Sadler, K. More Frequent, Longer, and Hotter Heat Waves for Australia in the Twenty-First Century. *J. Clim.* **2014**, *27*, 5851–5871. [[CrossRef](#)]
10. Schoetter, R.; Cattiaux, J.; Douville, H. Changes of western European heat wave characteristics projected by the CMIP5 ensemble. *Clim. Dyn.* **2014**, *45*, 1601–1616. [[CrossRef](#)]
11. Chaves, M.M.; Zarrouk, O.; Francisco, R.; Costa, J.M.; Santos, T.; Regalado, A.P.; Rodrigues, M.L.; Lopes, C.M. Grapevine under deficit irrigation: Hints from physiological and molecular data. *Ann. Bot.* **2010**, *105*, 661–676. [[CrossRef](#)]
12. Bonada, M.; Sadras, V.; Fuentes, S. Effect of elevated temperature on the onset and rate of mesocarp cell death in berries of Shiraz and Chardonnay and its relationship with berry shrivel. *Aust. J. Grape Wine Res.* **2013**, *19*, 87–94. [[CrossRef](#)]
13. Xiao, Z.; Liao, S.; Rogiers, S.; Sadras, V.; Tyerman, S. Effect of water stress and elevated temperature on hypoxia and cell death in the mesocarp of Shiraz berries. *Aust. J. Grape Wine Res.* **2018**, *24*, 487–497. [[CrossRef](#)]

14. Sadras, V.; Moran, M.; Bonada, M. Effects of elevated temperature in grapevine. I Berry sensory traits. *Aust. J. Grape Wine Res.* **2012**, *19*, 95–106. [CrossRef]
15. Zhang, P.; Howell, K.; Krstic, M.; Herderich, M.; Barlow, E.W.R.; Fuentes, S. Environmental factors and seasonality affect the concentration of rotundone in *Vitis vinifera* L. cv. Shiraz wine. *PLoS ONE* **2015**, *10*, e0133137. [CrossRef] [PubMed]
16. Rashid, M.A.; Andersen, M.N.; Wollenweber, B.; Kørup, K.; Zhang, X.; Olesen, J.E. Impact of heat-wave at high and low VPD on photosynthetic components of wheat and their recovery. *Environ. Exp. Bot.* **2018**, *147*, 138–146. [CrossRef]
17. Bhusal, N.; Han, S.-G.; Yoon, T.-M. Impact of drought stress on photosynthetic response, leaf water potential, and stem sap flow in two cultivars of bi-leader apple trees (*Malus × domestica* Borkh.). *Sci. Hortic.* **2019**, *246*, 535–543. [CrossRef]
18. Gambetta, G.A.; Herrera, J.C.; Dayer, S.; Feng, Q.; Hochberg, U.; Castellarin, S.D. The physiology of drought stress in grapevine: Towards an integrative definition of drought tolerance. *J. Exp. Bot.* **2020**, *71*, 4658–4676. [CrossRef]
19. Min, Z.; Li, R.; Chen, L.; Zhang, Y.; Li, Z.; Liu, M.; Ju, Y.; Fang, Y. Alleviation of drought stress in grapevine by foliar-applied strigolactones. *Plant Physiol. Biochem.* **2019**, *135*, 99–110. [CrossRef]
20. Mittler, R. Abiotic stress, the field environment and stress combination. *Trends Plant Sci.* **2006**, *11*, 15–19. [CrossRef]
21. Jing, B.; Shah, F.; Xiao, E.; Coulter, J.A.; Wu, W. Sprinkler irrigation increases grain yield of sunflower without enhancing the risk of root lodging in a dry semi-humid region. *Agric. Water Manag.* **2020**, *239*, 106270. [CrossRef]
22. Gilbert, D.E.; Meyer, J.L.; Kissler, J.J.; La Vine, P.D.; Carlson, C.V. Evaporation cooling of vineyards. *Calif. Agric.* **1970**, *24*, 12–14. [CrossRef]
23. Pagay, V.; Tyerman, S.; Jeffery, D.; Muhlack, R.; McCarthy, M.; Boss, P. *Using in-Canopy Misters to Mitigate the Negative Effects of Heatwaves in Grapevines*; Final Report to Wine Australia; 2018; Available online: <https://www.wineaustralia.com/research/projects/using-in-canopy-misters-to-mitigate-the> (accessed on 10 September 2021).
24. Edwards, E.; Smithson, L.; Graham, D.; Clingeffer, P. Grapevine canopy response to a high-temperature event during deficit irrigation. *Aust. J. Grape Wine Res.* **2011**, *17*, 153–161. [CrossRef]
25. Sousa, T.A.; Oliveira, M.T.; Moutinho-Pereira, J. Physiological indicators of plant water status of irrigated and non-irrigated grapevines grown in a low rainfall area of Portugal. *Plant Soil* **2006**, *282*, 127–134. [CrossRef]
26. Girona, J.; Mata, M.; del Campo, J.; Arbonés, A.; Bartra, E.; Marsal, J. The use of midday leaf water potential for scheduling deficit irrigation in vineyards. *Irrig. Sci.* **2006**, *24*, 115–127. [CrossRef]
27. Cogato, A.; Meggio, F.; Collins, C.; Marinello, F. Medium-resolution multispectral data from Sentinel-2 to assess the damage and the recovery time of late frost on vineyards. *Remote Sens.* **2020**, *12*, 1896. [CrossRef]
28. Poblete, T.; Ortega-Farías, S.; Moreno, M.A.; Bardeen, M. Artificial neural network to predict vine water status spatial variability using multispectral information obtained from an unmanned aerial vehicle (UAV). *Sensors* **2017**, *17*, 2488. [CrossRef]
29. Zarco-Tejada, P.J.; Ustin, S.; Whiting, M.L. Temporal and spatial relationships between within-field yield variability in cotton and high-spatial hyperspectral remote sensing imagery. *Agron. J.* **2005**, *97*, 641–653. [CrossRef]
30. Cogato, A.; Pezzuolo, A.; Sørensen, C.G.; De Bei, R.; Sozzi, M.; Marinello, F. A GIS-based multicriteria index to evaluate the mechanisability potential of Italian vineyard area. *Land* **2020**, *9*, 469. [CrossRef]
31. Mirás-Avalos, J.M.; Pérez-Sarmiento, F.; Alcobendas, R.; Alarcón, J.J.; Mounzer, O.; Nicolás, E. Using midday stem water potential for scheduling deficit irrigation in mid-late maturing peach trees under Mediterranean conditions. *Irrig. Sci.* **2016**, *34*, 161–173. [CrossRef]
32. Choné, X.; Van Leeuwen, C.; Dubourdieu, D.; Gaudillère, J.P. Stem water potential is a sensitive indicator of grapevine water status. *Ann. Bot.* **2001**, *87*, 477–483. [CrossRef]
33. Prieto, J.A.; Lebon, É.; Ojeda, H. Stomatal behavior of different grapevine cultivars in response to soil water status and air water vapor pressure deficit. *J. Int. Sci. Vigne Vin* **2010**, *44*, 9–20. [CrossRef]
34. Santesteban, L.G.; Miranda, C.; Royo, J.B. Effect of water deficit and rewatering on leaf gas exchange and transpiration decline of excised leaves of four grapevine (*Vitis vinifera* L.) cultivars. *Sci. Hortic.* **2009**, *121*, 434–439. [CrossRef]
35. Tomás, M.; Medrano, H.; Escalona, J.M.; Martorell, S.; Pou, A.; Ribas-Carbo, M.; Flexas, J. Variability of water use efficiency in grapevines. *Environ. Exp. Bot.* **2014**, *103*, 148–157. [CrossRef]
36. Greer, D.H.; Weston, C. Heat stress affects flowering, berry growth, sugar accumulation and photosynthesis of *Vitis vinifera* cv. Semillon grapevines grown in a controlled environment. *Funct. Plant Biol.* **2010**, *37*, 206–214. [CrossRef]
37. Zarco-Tejada, P.J.; Berjón, A.; López-Lozano, R.; Miller, J.R.; Martín, P.; Cachorro, V.; González, M.R.; De Frutos, A. Assessing vineyard condition with hyperspectral indices: Leaf and canopy reflectance simulation in a row-structured discontinuous canopy. *Remote Sens. Environ.* **2005**, *99*, 271–287. [CrossRef]
38. Rouse, J.; Haas, R.; Schell, J.; Deering, D.; Harlan, J. *Monitoring the Vernal Advancement and Retrogradation (Greenwave Effect) of Natural Vegetation*; Type III Final Report; NASA/GSFC: Greenbelt, MD, USA, 1974; p. 371.
39. Acevedo-Opazo, C.; Tisseyre, B.; Guillaume, S.; Ojeda, H. Test of NDVI information for a relevant vineyard zoning related to vine water status. In Proceedings of the VI European Conference on Precision Agriculture (ECPA), Skiathos, Greece, 3–6 June 2007; pp. 547–554.
40. Acevedo-Opazo, C.; Tisseyre, B.; Guillaume, S.; Ojeda, H. The potential of high spatial resolution information to define within-vineyard zones related to vine water status. *Precis. Agric.* **2008**, *9*, 285–302. [CrossRef]
41. Baluja, J.; Diago, M.P.; Balda, P.; Zorer, R.; Meggio, F.; Morales, F.; Tardaguila, J. Assessment of vineyard water status variability by thermal and multispectral imagery using an unmanned aerial vehicle (UAV). *Irrig. Sci.* **2012**, *30*, 511–522. [CrossRef]

42. Espinoza, C.Z.; Khot, L.R.; Sankaran, S.; Jacoby, P.W. High resolution multispectral and thermal remote sensing-based water stress assessment in subsurface irrigated grapevines. *Remote Sens.* **2017**, *9*, 961. [CrossRef]
43. Serrano, L.; González-Flor, C.; Gorchs, G. Assessing vineyard water status using the reflectance based Water Index. *Agric. Ecosyst. Environ.* **2010**, *139*, 490–499. [CrossRef]
44. Zarco-Tejada, P.J.; Gonzalez-Dugo, V.; Williams, L.; Suárez, L.; Jimenez-Berni, J.A.; Goldhamer, D.; Fereres, E. A PRI-based water stress index combining structural and chlorophyll effects: Assessment using diurnal narrow-band airborne imagery and the CWSI thermal index. *Remote Sens. Environ.* **2013**, *138*, 38–50. [CrossRef]
45. Di Gennaro, S.F.; Matese, A.; Gioli, B.; Toscano, P.; Zaldei, A.; Palliotti, A.; Genesio, L. Multisensor approach to assess vineyard thermal dynamics combining high-resolution unmanned aerial vehicle (UAV) remote sensing and wireless sensor network (WSN) proximal sensing. *Sci. Hortic.* **2017**, *221*, 83–87. [CrossRef]
46. Gitelson, A.A.; Viña, A.; Ciganda, V.; Rundquist, D.C.; Arkebauer, T.J. Remote estimation of canopy chlorophyll content in crops. *Geophys. Res. Lett.* **2005**, *32*, 1–4. [CrossRef]
47. Chen, J.M. Evaluation of vegetation indices and a modified simple ratio for boreal applications. *Can. J. Remote Sens.* **1996**, *22*, 229–242. [CrossRef]
48. Haboudane, D.; Miller, J.R.; Tremblay, N.; Zarco-Tejada, P.J.; Dextraze, L. Integrated narrow-band vegetation indices for prediction of crop chlorophyll content for application to precision agriculture. *Remote Sens. Environ.* **2002**, *81*, 416–426. [CrossRef]
49. Courel, M.-F.; Chamard, P.; Guenegou, M.J.; Lerhun, J.; Lévassieur, M.; Togola, M. Utilisation des bandes spectrales du vert et du rouge pour une meilleure évaluation des formations végétales actives. In Proceedings of the Congrès AUPELF-UREF, Sherbrooke, QC, Canada, 21–23 October 1991; pp. 203–210.
50. Jordan, C.F. Derivation of leaf-area index from quality of light on the forest floor. *Ecology* **1969**, *50*, 663–666. [CrossRef]
51. Gitelson, A.A.; Kaufman, Y.J.; Stark, R.; Rundquist, D. Novel algorithms for remote estimation of vegetation fraction. *Remote Sens. Environ.* **2002**, *80*, 76–87. [CrossRef]
52. Pôças, I.; Rodrigues, A.; Gonçalves, S.; Costa, P.M.; Gonçalves, I.; Pereira, L.S.; Cunha, M. Predicting grapevine water status based on hyperspectral reflectance vegetation indices. *Remote Sens.* **2015**, *7*, 16460–16479. [CrossRef]
53. Gamon, J.A.; Peñuelas, J.; Field, C.B. A narrow-waveband spectral index that tracks diurnal changes in photosynthetic efficiency. *Remote Sens. Environ.* **1992**, *41*, 35–44. [CrossRef]
54. Liu, H.Q.; Huete, A. A feedback based modification of the NDVI to minimize canopy background and atmospheric noise. *IEEE Trans. Geosci. Remote Sens.* **1995**, *33*, 457–465. [CrossRef]
55. Cheng, Y.-B.; Zarco-Tejada, P.J.; Riano, D.; Rueda, C.A.; Ustin, S. Estimating vegetation water content with hyperspectral data for different canopy scenarios: Relationships between AVIRIS and MODIS indexes. *Remote Sens. Environ.* **2006**, *105*, 354–366. [CrossRef]
56. Dold, C.; Heitman, J.; Giese, G.; Howard, A.; Havlin, J.; Sauer, T. Upscaling Evapotranspiration with parsimonious models in a North Carolina vineyard. *Agronomy* **2019**, *9*, 152. [CrossRef]
57. Penuelas, J.; Filella, I.; Biel, C.; Serrano, L.; Savé, R. The reflectance at the 950–970 nm region as an indicator of plant water status. *Int. J. Remote Sens.* **1993**, *14*, 1887–1905. [CrossRef]
58. Fórián, T.; Nagy, A.; Riczu, P.; Mézes, L.; Tamás, J. Vineyards characteristic by using GIS and reflectance measurements on the Nagy-Eged hill in Hungary. *Int. J. Hortic. Sci.* **2016**, *18*, 57–60. [CrossRef]
59. Thenkabail, P.S.; Enclona, E.A.; Ashton, M.S.; Van Der Meer, B. Accuracy assessments of hyperspectral waveband performance for vegetation analysis applications. *Remote Sens. Environ.* **2004**, *91*, 354–376. [CrossRef]
60. Ray, S.S.; Singh, J.P.; Panigraphy, S. Use of hyperstrectralremote senings data for crop stress detection: Ground-based studies. *Int. Arch. Photogram. Remote. Sens. Spat. Inf. Sci.* **2010**, *38*, 562–570.
61. Mutanga, O.; Skidmore, A.; Prins, H. Predicting in situ pasture quality in the Kruger National Park, South Africa, using continuum-removed absorption features. *Remote Sens. Environ.* **2004**, *89*, 393–408. [CrossRef]
62. Huete, A.R.; Liu, H.Q.; van Leeuwen, W.J.D. The use of vegetation indices in forested regions: Issues of linearity and saturation. *Int. Geosci. Remote Sens. Symp.* **1997**, *4*, 1966–1968.
63. Kassambara, A.; Mundt, F. Factoextra: Extract and Visualize the Results of Multivariate Data Analyses (Versión 1.0.5). Available online: <https://cran.r-project.org/package=factoextra> (accessed on 1 March 2021).
64. Ruiz, E.; Jackson, S.; Cimentada, J. Corrr: Correlations in R. Available online: <https://cran.r-project.org/web/packages/corrr/index.htm> (accessed on 1 March 2021).
65. Dormann, C.F.; Elith, J.; Bacher, S.; Buchmann, C.; Carl, G.; Carré, G.; Marquéz, J.R.G.; Gruber, B.; Lafourcade, B.; Leitão, P.J.; et al. Collinearity: A review of methods to deal with it and a simulation study evaluating their performance. *Ecography* **2013**, *36*, 27–46. [CrossRef]
66. Yang, J.; Yang, J.Y. Why can LDA be performed in PCA transformed space? *Pattern Recognit.* **2003**, *36*, 563–566. [CrossRef]
67. Roever, C.; Raabe, N.; Luebke, K.; Ligges, U.; Szepannek, G.; Zentgraf, M. klaR: Classification and visualization. Available online: <https://cran.r-project.org/package=klaR> (accessed on 1 March 2021).
68. Greer, D.H.; Weedon, M. Modelling photosynthetic responses to temperature of grapevine (*Vitis vinifera* cv. Semillon) leaves on vines grown in a hot climate. *Plant Cell Environ.* **2011**, *35*, 1050–1064. [CrossRef]
69. Zsófi, Z.; Gál, L.; Szilágyi, Z.; Szűcs, E.; Marschall, M.; Nagy, Z.; Bálo, B. Use of stomatal conductance and pre-dawn water potential to classify terroir for the grape variety Kékfrankos. *Aust. J. Grape Wine Res.* **2009**, *15*, 36–47. [CrossRef]

70. Pagay, V.; Canela, F.; Bennet, C. *How Does Phenological Stage Influence Grapevine Water Requirements for Shiraz and Chardonnay in the Riverland?* Final Report to Wine Australia; 2021; Available online: <https://www.growag.com/listings/research-project/incubator-initiative-how-does-phenological-stage-influence-grapevine-water-requirements-for-shiraz-and-chardonnay-in-the-riverland> (accessed on 10 September 2021).
71. Acevedo-Opazo, C.; Ortega-Farias, S.; Fuentes, S. Effects of grapevine (*Vitis vinifera* L.) water status on water consumption, vegetative growth and grape quality: An irrigation scheduling application to achieve regulated deficit irrigation. *Agric. Water Manag.* **2010**, *97*, 956–964. [[CrossRef](#)]
72. Pierantozzi, P.; Torres, M.; Bodoira, R.; Maestri, D. Water relations, biochemical–physiological and yield responses of olive trees (*Olea europaea* L. cvs. Arbequina and Manzanilla) under drought stress during the pre-flowering and flowering period. *Agric. Water Manag.* **2013**, *125*, 13–25. [[CrossRef](#)]
73. Bhusal, N.; Lee, M.; Lee, H.; Adhikari, A.; Han, A.R.; Kim, H.S. Evaluation of morphological, physiological, and biochemical traits for assessing drought resistance in eleven tree species. *Sci. Total. Environ.* **2021**, *779*, 146466. [[CrossRef](#)] [[PubMed](#)]
74. Brito, C.; Dinis, L.-T.; Moutinho-Pereira, J.; Correia, C.M.; Pereira, M. Drought stress effects and olive tree acclimation under a changing climate. *Plants* **2019**, *8*, 232. [[CrossRef](#)]
75. Patakas, A.; Noitsakis, B.; Chouzouri, A. Optimization of irrigation water use in grapevines using the relationship between transpiration and plant water status. *Agric. Ecosyst. Environ.* **2005**, *106*, 253–259. [[CrossRef](#)]
76. Patakas, A.; Noitsakis, B.; Stavrakas, D. Adaptation of leaves of *Vitis vinifera* L. to seasonal drought as affected by leaf age. *Vitis* **1997**, *36*, 11–14.
77. Rapaport, T.; Hochberg, U.; Shoshany, M.; Karnieli, A.; Rachmilevitch, S. Combining leaf physiology, hyperspectral imaging and partial least squares-regression (PLS-R) for grapevine water status assessment. *ISPRS J. Photogramm. Remote Sens.* **2015**, *109*, 88–97. [[CrossRef](#)]
78. Palliotti, A.; Poni, S. Grapevine under light and heat stresses. In *Grapevine in a Changing Environment*; Wiley: Hoboken, NJ, USA, 2015; pp. 148–178.
79. Urban, J.; Ingwers, M.W.; McGuire, M.A.; Teskey, R.O. Increase in leaf temperature opens stomata and decouples net photosynthesis from stomatal conductance in *Pinus taeda* and *Populus deltoides* × *nigra*. *J. Exp. Bot.* **2017**, *68*, 1757–1767. [[CrossRef](#)]
80. Flexas, J.; Galmés, J.; Gallé, A.; Gulías, J.; Pou, A.; Ribas-Carbo, M.; Tomàs, M.; Medrano, H. Improving water use efficiency in grapevines: Potential physiological targets for biotechnological improvement. *Aust. J. Grape Wine Res.* **2010**, *16*, 106–121. [[CrossRef](#)]
81. Bchir, A.; Escalona, J.M.; Gallé, A.; Hernández-Montes, E.; Tortosa, I.; Braham, M.; Medrano, H. Carbon isotope discrimination ($\delta^{13}C$) as an indicator of vine water status and water use efficiency (WUE): Looking for the most representative sample and sampling time. *Agric. Water Manag.* **2016**, *167*, 11–20. [[CrossRef](#)]
82. Luo, H.-B.; Ma, L.; Xi, H.-F.; Duan, W.; Li, S.-H.; Loescher, W.; Wang, J.-F.; Wang, L.-J. Photosynthetic responses to heat treatments at different temperatures and following recovery in grapevine (*Vitis amurensis* L.) leaves. *PLoS ONE* **2011**, *6*, e23033. [[CrossRef](#)]
83. Bauer, H. Photosynthesis of Ivy Leaves (*Hedera helix*) after Heat Stress I. CO₂-Gas Exchange and diffusion resistances. *Physiol. Plant* **1978**, *44*, 400–406. [[CrossRef](#)]
84. Peñuelas, J.; Filella, L. Visible and near-infrared reflectance techniques for diagnosing plant physiological status. *Trends Plant Sci.* **1998**, *3*, 151–156. [[CrossRef](#)]
85. Usman, M.G.; Rafii, M.Y.; Ismail, M.R.; Malek, M.A.; Latif, M.A.; Oladosu, Y. Heat shock proteins: Functions and response against heat stress in plants. *Int. J. Sci. Technol. Res.* **2014**, *3*, 204–218.
86. Wang, L.-J.; Fan, L.; Loescher, W.; Duan, W.; Liu, G.-J.; Cheng, J.-S.; Luo, H.-B.; Li, S.-H. Salicylic acid alleviates decreases in photosynthesis under heat stress and accelerates recovery in grapevine leaves. *BMC Plant Biol.* **2010**, *10*, 34. [[CrossRef](#)]
87. Zarco-Tejada, P.J.; Jimenez-Berni, J.A.; Suárez, L.; Sepulcre-Cantó, G.; Morales, F.; Miller, J.R. Imaging chlorophyll fluorescence with an airborne narrow-band multispectral camera for vegetation stress detection. *Remote Sens. Environ.* **2009**, *113*, 1262–1275. [[CrossRef](#)]
88. Perry, E.M.; Roberts, D.A. Sensitivity of narrow-band and broad-band indices for assessing nitrogen availability and water stress in an annual crop. *Agron. J.* **2008**, *100*, 1211–1219. [[CrossRef](#)]
89. Romero, M.; Luo, Y.; Su, B.; Fuentes, S. Vineyard water status estimation using multispectral imagery from an UAV platform and machine learning algorithms for irrigation scheduling management. *Comput. Electron. Agric.* **2018**, *147*, 109–117. [[CrossRef](#)]
90. Xiao, F.; Yang, Z.Q.; Lee, K.W. Photosynthetic and physiological responses to high temperature in grapevine (*Vitis vinifera* L.) leaves during the seedling stage. *J. Hortic. Sci. Biotechnol.* **2016**, *92*, 2–10. [[CrossRef](#)]
91. Dobrowski, S.; Pushnik, J.; Zarco-Tejada, P.J.; Ustin, S. Simple reflectance indices track heat and water stress-induced changes in steady-state chlorophyll fluorescence at the canopy scale. *Remote Sens. Environ.* **2005**, *97*, 403–414. [[CrossRef](#)]
92. Sonmez, N.K.; Emekli, Y.; Sari, M.; Bastug, R.; Sari, M. Relationship between spectral reflectance and water stress conditions of Bermuda grass (*Cynodon dactylon* L.). *N. Z. J. Agric. Res.* **2008**, *51*, 223–233. [[CrossRef](#)]
93. Houborg, R.; Soegaard, H.; Boegh, E. Combining vegetation index and model inversion methods for the extraction of key vegetation biophysical parameters using Terra and Aqua MODIS reflectance data. *Remote Sens. Environ.* **2007**, *106*, 39–58. [[CrossRef](#)]
94. Rodríguez-Pérez, J.R.; Riaño, D.; Carlisle, E.; Ustin, S.; Smart, D.R. Evaluation of hyperspectral reflectance indexes to detect grapevine water status in vineyards. *Am. J. Enol. Vitic.* **2007**, *58*, 302–317.

-
95. De Jong, S.; Addink, E.; Hoogenboom, P.; Nijland, W. The spectral response of *Buxus sempervirens* to different types of environmental stress—A laboratory experiment. *ISPRS J. Photogramm. Remote Sens.* **2012**, *74*, 56–65. [[CrossRef](#)]
 96. Wang, J.; Xu, R.; Yang, S. Estimation of plant water content by spectral absorption features centered at 1450 nm and 1940 nm regions. *Environ. Monit. Assess.* **2008**, *157*, 459–469. [[CrossRef](#)] [[PubMed](#)]